Electronic Supplementary Material (ESI) for Journal of Materials Chemistry A.

Supporting Information

for

Triple atom catalyst with ultrahigh loading potential for nitrogen electrochemical reduction

Zhi Wen Chen,[1] Li Xin Chen,[2] Ming Jiang,[2] Dachang Chen,[2] Zhi Li Wang,[1] Xue Yao, Chandra Veer Singh,*[2, 3] Qing Jiang*[1]

[1]*Key Laboratory of Automobile Materials, Ministry of Education, and School of Materials Science and Engineering, Jilin University, Changchun 130022, China*

[2]*Department of Materials Science and Engineering, University of Toronto, 184 College Street, Suite 140, Toronto, ON M5S 3E4, Canada.*

[3]*Department of Mechanical and Industrial Engineering, University of Toronto, 5 King's College Road, Toronto, ON M5S 3G8, Canada.*

*Correspondence and requests for materials should be addressed to C. V. Singh (chandraveer.singh@utoronto.ca) or Q. Jiang (jiangq@jlu.edu.cn).

Table S1. Total energy and binding energy of GDY/Gra with different lattice constants.

Lattice constant (Å)	Total energy (Ha)	Binding energy (eV)
19.68	-7615.0704591	-7.695
19.29	-7615.0676086	-7.695
18.90	-7614.9228224	-7.675

Table S2. Reaction free energy of the potential limiting step ($NH^* + H^+ + e^- \rightarrow NH_2^*$) of NRR on Fe_3-GDY/Gra with solvation effect and dipole correction.

Methods	ΔG ($NH^* + H^+ + e^- \rightarrow NH_2^*$, eV)
GGA-PBE	0.370
Solvation model+dipole correction	0.439

Table S3. Spin polarization, charge transfer, and the length of N-N bond for Fe_x-GDY/Gra, N_2^*, and NNH*.

Systems	Spin	Charge	Bond length (Å)
Fe_1-GDY/Gra	2.370	~	~
N_2^*(Fe_1-GDY/Gra)	2.149	0.027	1.12
NNH*(Fe_1-GDY/Gra)	1.352	-0.066	1.20
Fe_2-GDY/Gra	5.307	~	~
N_2^*(Fe_2-GDY/Gra)	4.350	-0.060	1.18
NNH*(Fe_2-GDY/Gra)	3.640	-0.119	1.26
Fe_3-GDY/Gra	6.848	~	~
N_2^*(Fe_3-GDY/Gra)	5.076	-0.125	1.22
NNH*(Fe_3-GDY/Gra)	4.007	-0.134	1.29

Table S4. Potential limiting steps (PLS) and their reaction free energy values (ΔG, eV) of M_x-GDY/Gra (M = Mn, Fe, Co, Ni; x = 1, 2, 3) with low loading.

M_x-GDY/Gra	PLS	ΔG (eV)
Mn_1-GDY/Gra	$N_2^* + H^+ + e^- \rightarrow N_2H^*$	1.00
Fe_1-GDY/Gra	$N_2^* + H^+ + e^- \rightarrow N_2H^*$	1.06
Co_1-GDY/Gra	$N_2^* + H^+ + e^- \rightarrow N_2H^*$	1.46
Ni_1-GDY/Gra	$NNH_2^* + H^+ + e^- \rightarrow N^* + NH_3$	1.76
Mn_2-GDY/Gra	$NH_2^* + H^+ + e^- \rightarrow * + NH_3$	1.46
Fe_2-GDY/Gra	$NH_2^* + H^+ + e^- \rightarrow * + NH_3$	1.37

Co_2-GDY/Gra	$NH_2^* + H^+ + e^- \rightarrow * + NH_3$	1.36
Ni_2-GDY/Gra	$N_2^* + H^+ + e^- \rightarrow N_2H^*$	1.05
Mn_3-GDY/Gra	$NH_2^* + H^+ + e^- \rightarrow * + NH_3$	0.55
Fe_3-GDY/Gra	$NH^* + H^+ + e^- \rightarrow NH_2^*$	0.37
Co_3-GDY/Gra	$NH_2^* + H^+ + e^- \rightarrow * + NH_3$	0.38
Ni_3-GDY/Gra	$N_2^* + H^+ + e^- \rightarrow N_2H^*$	1.01

Table S5. Comparisons of the mass loading of active atoms among some atomic catalysts (SACs, DACs, and TACs), note that the last one is a theoretical work.

Atomic Catalysts	Loading of Active Atoms	References
Fe_3-GDY/Gra-35.8	35.8 wt%	This work
Pt/CeO_2	1 wt%	43
FeN_4/GN	2.7 wt%	44
Pt/antimony-doped tin oxide	4 wt%	45
Co-MoS_2	1.8 wt%	46
Ru SAs/N-C	0.18 wt%	8
Pt_2/MoS_2	5 wt%	47
Fe_2/mpg-C_3N_4	0.15 wt%	15
FeCo/CNT	2.34 wt%	48
Ru_3/CN (Ru_1/CN)	0.10 wt% (0.23 wt%)	16
W_S-WS_2	4.5 wt%	49

Table S6. Theoretical mass loading of active metal atoms on M_x-GDY/Gra (M = Mn, Fe, Co, Ni; x = 1, 2, 3).

M_x-GDY/Gra	Theoretical mass Loading
Mn_1-GDY/Gra	15.5 wt%
Fe_1-GDY/Gra	15.7 wt%
Co_1-GDY/Gra	16.4 wt%
Ni_1-GDY/Gra	16.4 wt%
Mn_2-GDY/Gra	26.8 wt%
Fe_2-GDY/Gra	27.1 wt%
Co_2-GDY/Gra	28.2 wt%
Ni_2-GDY/Gra	28.1 wt%
Mn_3-GDY/Gra	35.4 wt%
Fe_3-GDY/Gra	35.8 wt%
Co_3-GDY/Gra	37.1 wt%
Ni_3-GDY/Gra	37.0 wt%

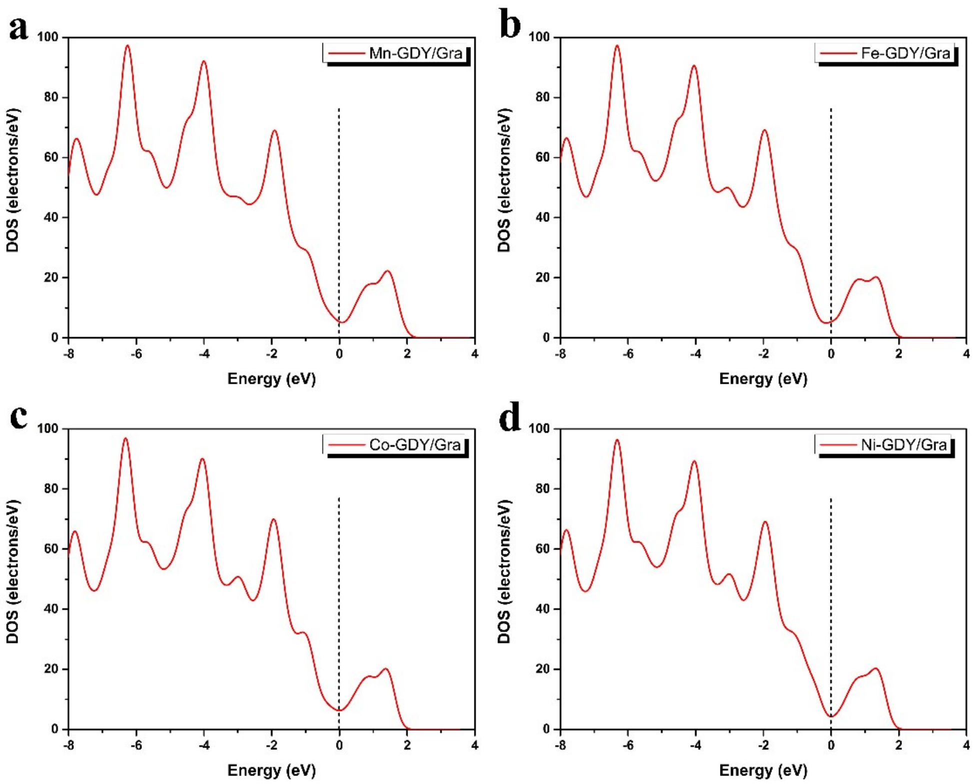

Figure S1. Density of states (DOS) of M-GDY/Gra (M = Mn, Fe, Co, and Ni). The black dotted line indicates the Fermi energy level.

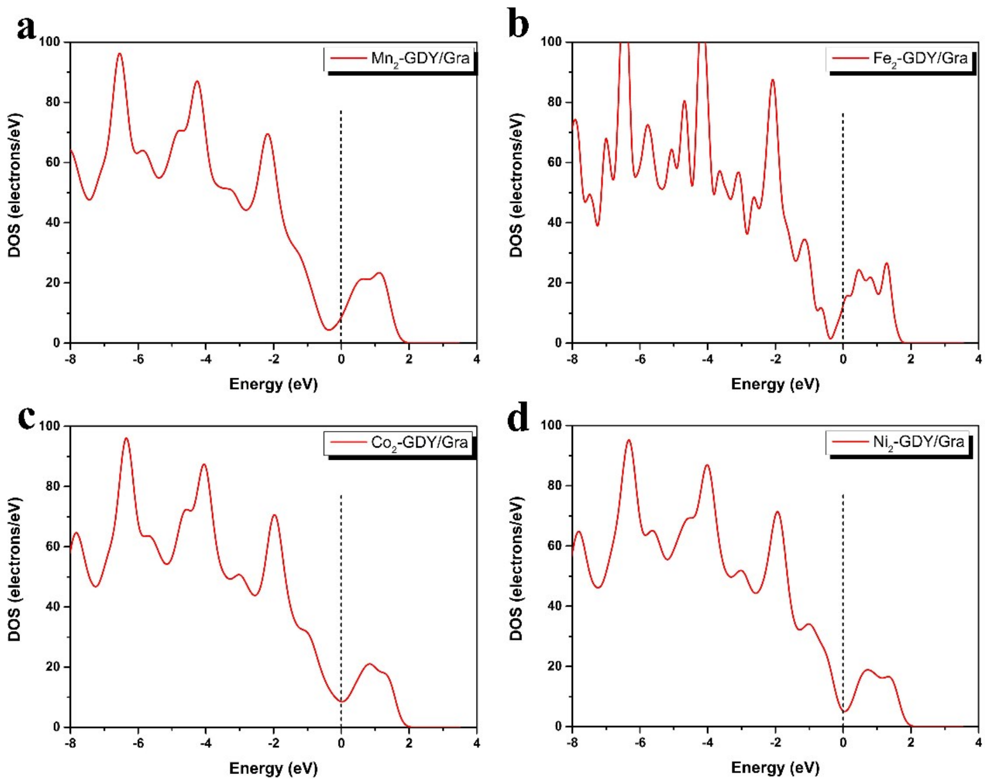

Figure S2. Density of states (DOS) of M_2-GDY/Gra (M = Mn, Fe, Co, and Ni). The black dotted line indicates the Fermi energy level.

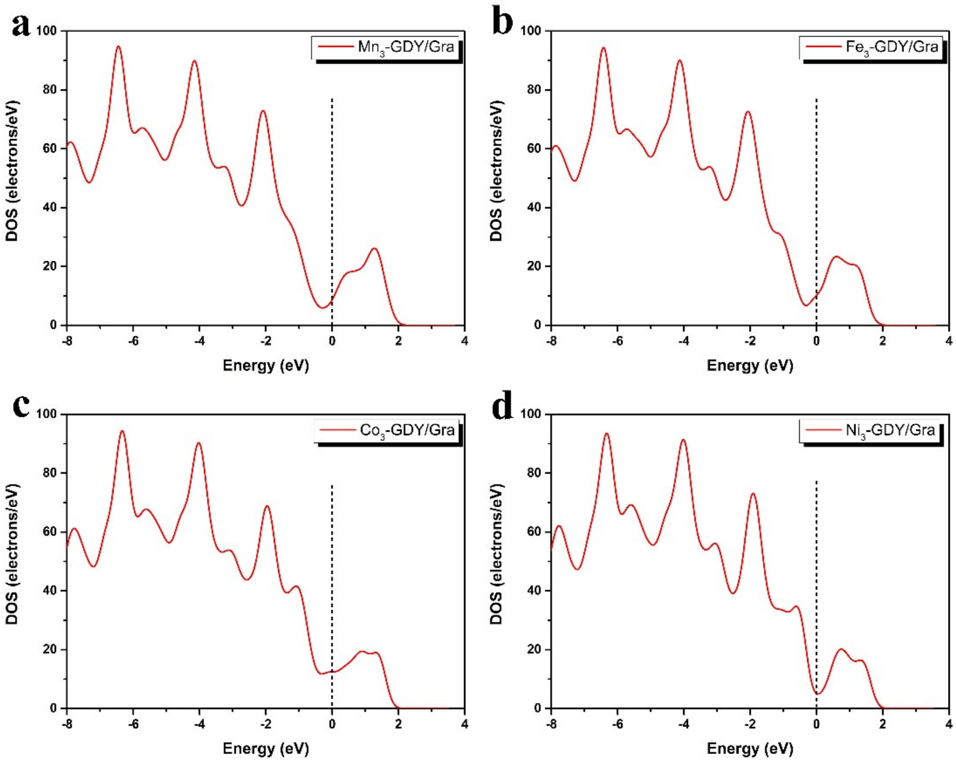

Figure S3. Density of states (DOS) of M_3-GDY/Gra (M = Mn, Fe, Co, and Ni). The black dotted line indicates the Fermi energy level.

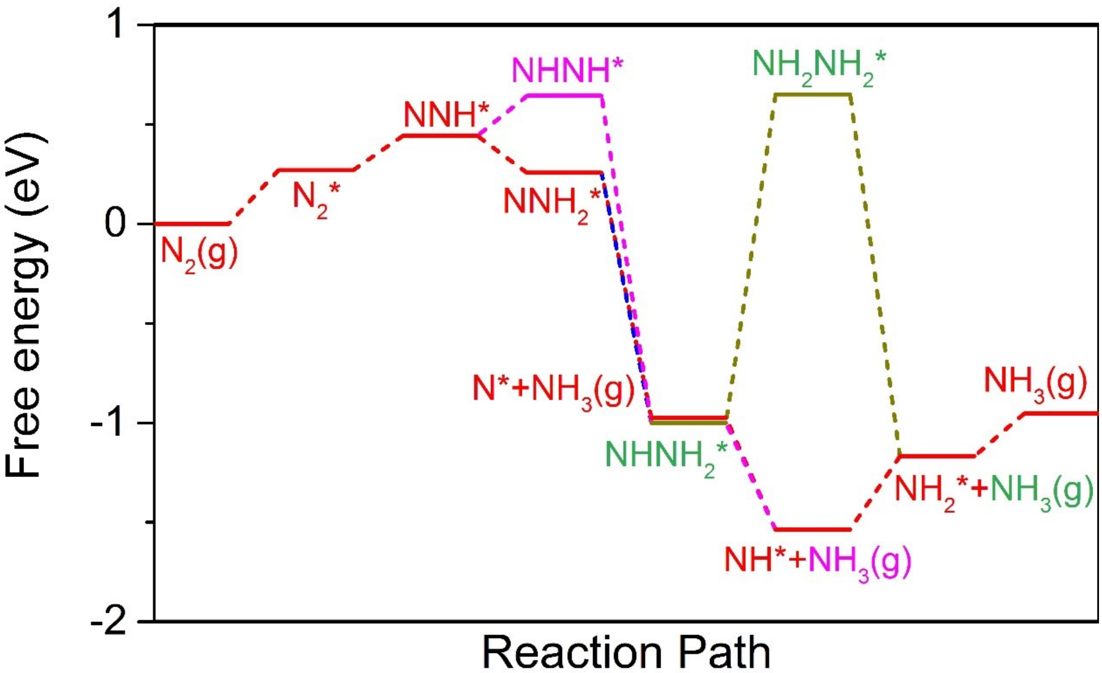

Figure S4. All possible reaction paths of NRR on Fe_3-GDY/Gra. The red line indicates the optimal reaction process.

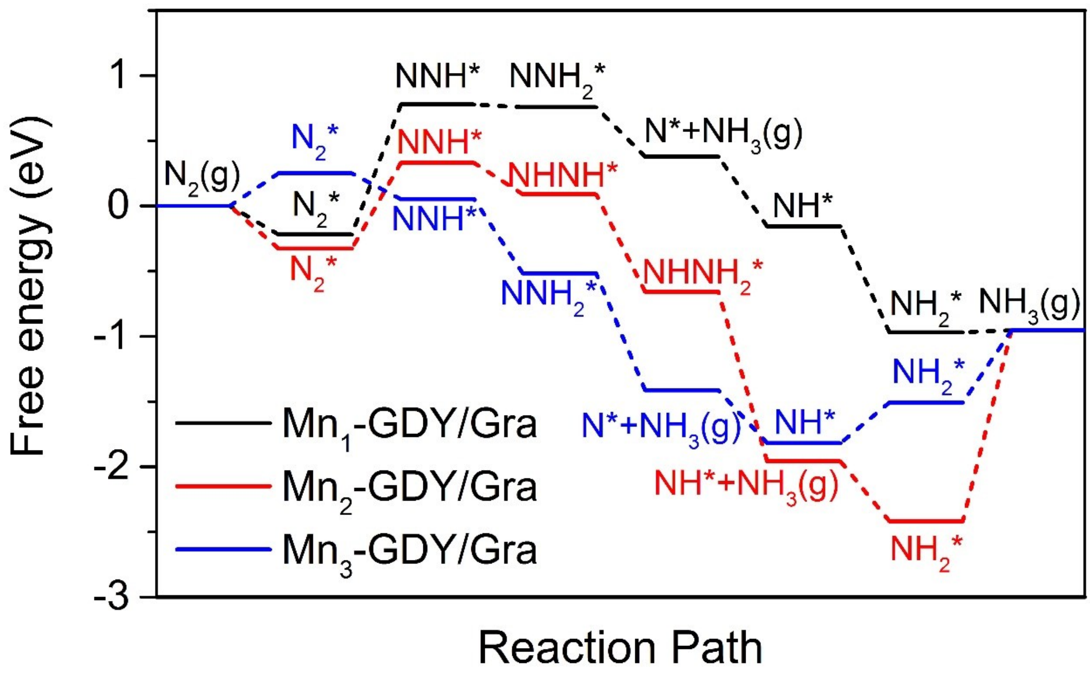

Figure S5. Reaction paths of NRR on Mn_x-GDY/Gra (x = 1, 2, 3).

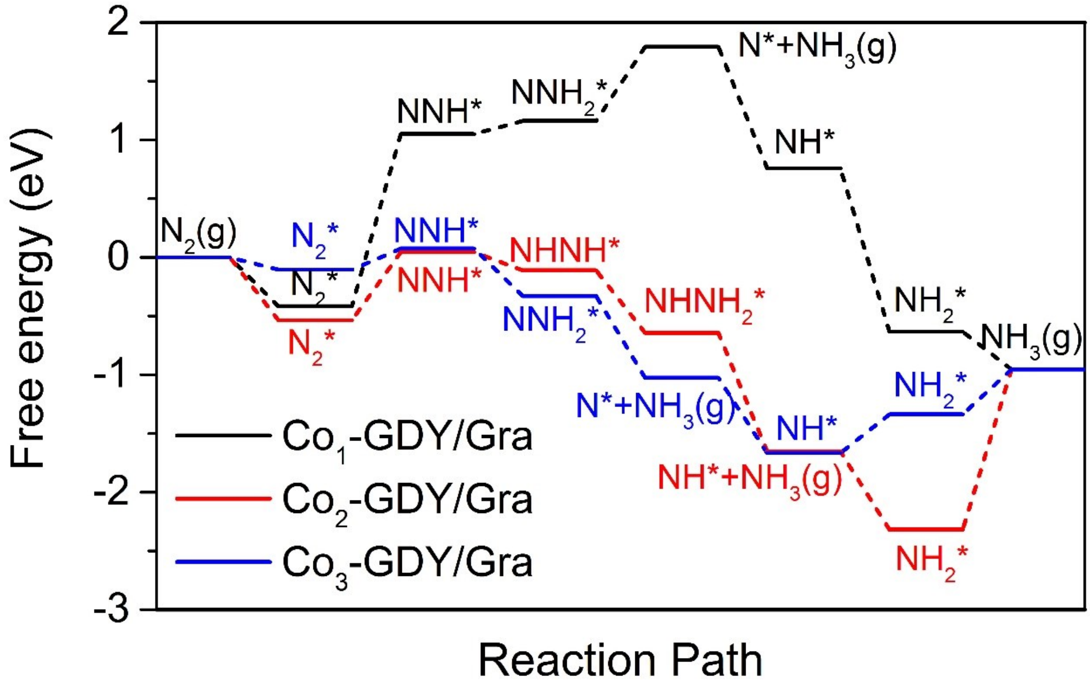

Figure S6. Reaction paths of NRR on Co_x-GDY/Gra (x = 1, 2, 3).

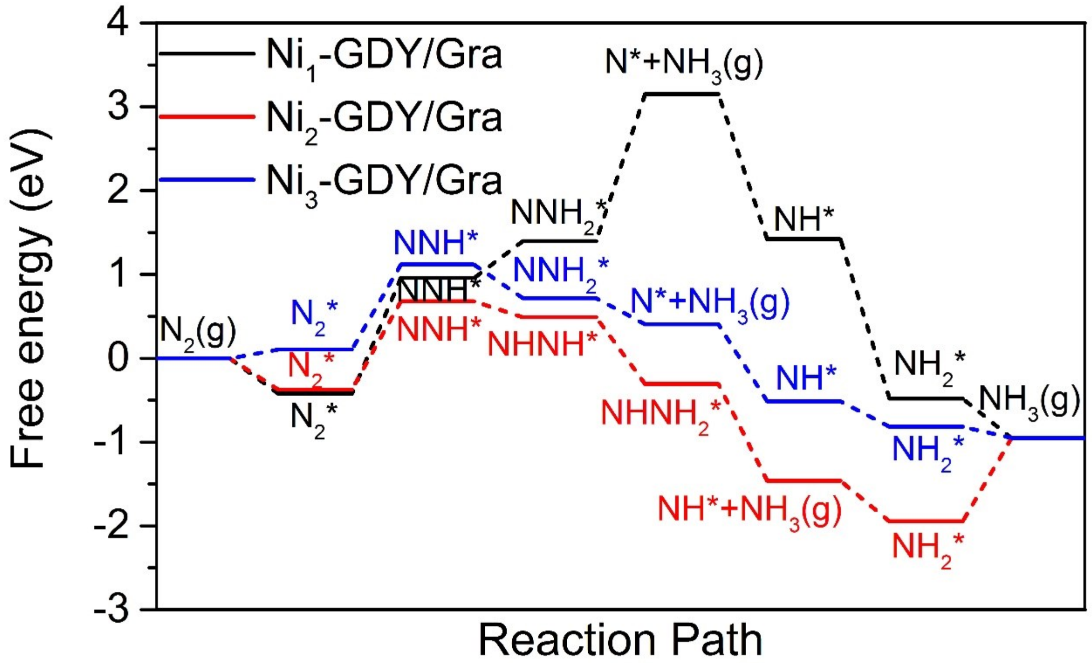

Figure S7. Reaction paths of NRR on Ni_x-GDY/Gra (x = 1, 2, 3).

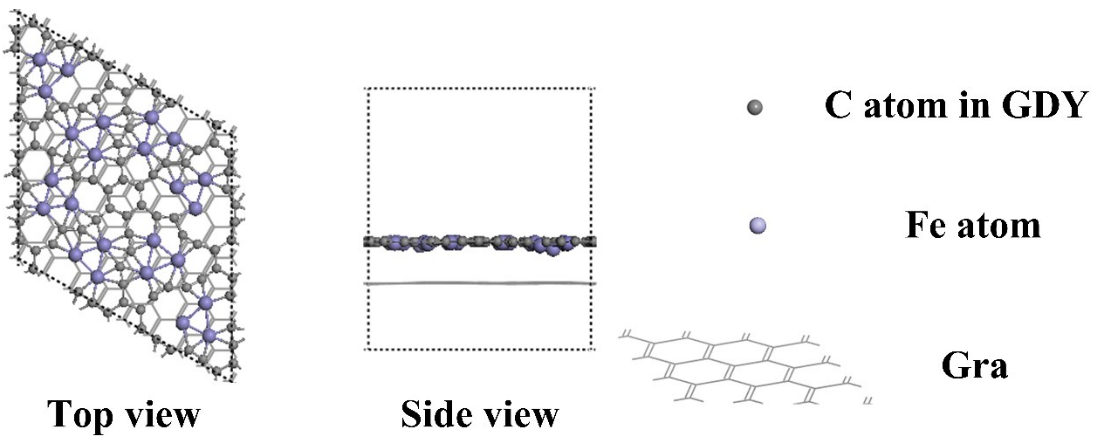

Figure S8. Geometric optimization structure (top and side views) of Fe_3-GDY/Gra-35.8.